# Optimizing and Comparing the Efficiencies of Relaxometry Sequences in Quantitative T1 and T2 Imaging

Yang Liu[1], John R. Buck[1], Shaokuan Zheng[2], and Vasiliki N. Ikonomidou[3]

[1]*Electrical and Computer Engineering, University of Massachusetts Dartmouth, North Dartmouth, MA, United States,* [2]*Department of Radiology, University of Massachusetts Medical School, Worcester, MA, United States,* [3]*Bioengineering, George Mason University, Fairfax, VA, United States*

**Target Audience:** Researchers and clinicians interested in quantitative MRI relaxometry sequences design

**Purpose:** Quantitative MRI estimates pixel-wise maps of MR quantities such as $T_1$ and $T_2$. These quantitative MR maps prove clinically useful in neurodegenerative pathology evaluations as well as brain anatomy and functional studies. Perturbation based sequences such as inversion recovery (IR)[1,2], saturation recovery (SR)[3] and Look-Locker (LL)[4] quantify $T_1$ information. Joint $T_1/T_2$ relaxometry sequences such as spin-echo inversion-recovery (SEIR)[5] and Driven Equilibrium Single Pulse Observation of $T_1/T_2$ (DESPOT)[6] simultaneously estimate $T_1$ and $T_2$. Estimating $T_1/T_2$ precisely (low variance) and accurately (low bias - difference between $T_1/T_2$ estimates and the true $T_1/T_2$) in a relatively short scan time is very desirable in this context. Although there is extensive relaxometry protocol design research for quantitative MRI, little effort has been made to explore and quantify the complete factors controlling the $T_1/T_2$ estimation efficiencies. This paper establishes a statistical framework to evaluate and compare different relaxometry sequences based on their $T_1/T_2$ estimation characteristics. This framework considers relaxometry protocols as estimation algorithms and proposes two new metrics: $T_1/T_2$-to-noise ratio (TNR) to characterize $T_1/T_2$ estimates' precisions and TNR efficiency to measure $T_1/T_2$ estimates' precision per unit time. The TNR and its efficiency are defined in terms of the Cramer-Rao Bound (CRB)[7], a statistical lower bound on the parameter estimate variance. This framework predicts the $T_1/T_2$ mapping performances of any relaxometry approaches before phantom or *in vivo* experiments.

**Methods:** The CRB, calculated as the inverse of Fisher information matrix (FIM), sets a lower bound on the variance of any unbiased parameter estimates for a given signal model. The FIM quantifies the signals' sensitivities to changes of $\theta = [M_0, T_1, T_2]$ in noisy measurements[7]. Assuming white Gaussian noise and complete knowledge of $B_0$ and $B_1$ inhomogeneity, Eq. 1 establishes a common CRB expression on $T_1/T_2$ estimations for any relaxometry approach. There are three components in the CRB expression: the *SNR* in Eq. 1b, the *sensitivity* of the signal vector $\mathbf{s}$ to $T_1/T_2$ (Sens in Eq. 1c) and the *orthogonality* between the signal vector $\mathbf{s}$ and the sensitivity vectors (Orth in Eq. 1d). The TNR in Eq. 2 describes a ratio between the true $T_1/T_2$ over the square root of the CRB and predicts the precisions of $T_1$ and $T_2$ estimates. The $\sqrt{T_{scan}/T_{seq}}$ factor represents the TNR improvement due to signal averaging in total scan time $T_{scan}$ when each $T_1/T_2$ estimate requires $T_{seq}$. The TNR efficiency $\Gamma$ follows from Eq. 2 by setting the $T_{scan}$ term to unity and replacing CRB with Eq. 1a. Eq. 3 reveals that the TNR efficiency depends linearly on the input SNR and the signals' sensitivity, both of which were often incorporated in prior sequence design research[6,8,9] studying MR parameter mapping efficiencies. However, no prior work recognized that improving the orthogonality between the signal vector $\mathbf{s}$ and the sensitivity vectors equally improves the $T_1/T_2$ estimate efficiency. This paper evaluates and compares the TNR efficiencies of the conventional IR[1], fast IR[2], SR[3] and LL[4] sequences for $T_1$ relaxometry, and the SEIR and DESPOT sequences for joint $T_1/T_2$ relaxometry. All sequence parameters were chosen to optimize the TNR efficiencies following a max-min criterion (Eq. 4) to guarantee the overall optimality of sequence parameters within the $T_1$ and $T_2$ ranges of interest. A reference range of $T_1 = [1000, 2000]$ ms and $T_2 = [60, 110]$ ms characterizes brain white matter (WM) and grey matter (GM)[10]. All sequence optimizations were implemented using the MATLAB2012a Optimization Toolbox 'fmincon'.

$$\mathrm{CRB}(\mathrm{T}) = (\mathrm{SNR}\cdot\mathrm{Sens}\cdot\mathrm{Orth})^{-2} \quad \text{Eq. 1}a; \qquad \mathrm{SNR} = M_0/\sigma \quad \text{Eq. 1b}; \qquad \mathrm{Sens} = \begin{cases} \|\partial \mathbf{s}/\partial T_1\|, \text{for } T_1 \text{ relaxometry} \\ \|\partial \mathbf{s}/\partial T_j\|, \text{for } T_1/T_2 \text{ relaxometry} \end{cases} \quad \text{Eq. 1c};$$

$$\mathrm{Orth} = \begin{cases} \sin\phi_1 & \text{for } T_1 \text{ relaxometry} \\ \sqrt{1 + 2\prod_{i=1}^{3}\cos\phi_i - \sum_{i=1}^{3}\cos^2\phi_i}\,/\,\sin\phi_{3-j} & \text{for } T_1/T_2 \text{ relaxometry} \end{cases}, \text{with } \begin{cases} \cos\phi_1 = <\mathbf{h},\ \partial\mathbf{h}/\partial T_1> \\ \cos\phi_2 = <\mathbf{h},\ \partial\mathbf{h}/\partial T_2> \\ \cos\phi_3 = <\partial\mathbf{h}/\partial T_1,\ \partial\mathbf{h}/\partial T_2> \end{cases} \quad \text{Eq. 1d};$$

$$\mathrm{TNR} = T_{1,2}\cdot \mathrm{CRB}^{-1/2}\cdot\sqrt{T_{scan}/T_{seq}} \quad \text{Eq. 2}; \qquad \text{TNR efficiency } \Gamma_j = T_j\cdot\mathrm{SNR}\cdot\mathrm{Sens}\cdot\mathrm{Orth}/\sqrt{T_{seq}},\ j = 1,2 \quad \text{Eq. 3};$$

$$(\mathbf{t},\boldsymbol{\alpha})^{\mathrm{opt}} = \arg\max_{\mathbf{t},\boldsymbol{\alpha}} \min_{\theta_{min}\le\theta\le\theta_{max}} \rho_1\Gamma_1 + (1-\rho_1)\Gamma_2, \text{ for } 0 \le \rho_1 \le 1 \quad \text{Eq. 4};$$

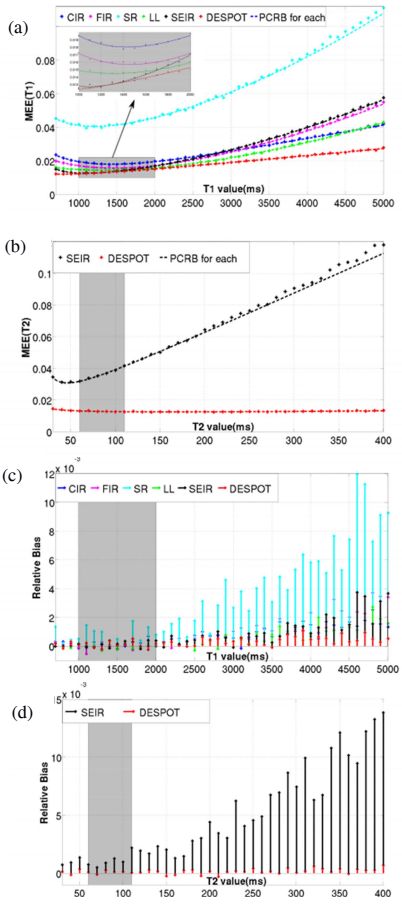


Fig.1 Monte Carlo simulated $T_1$ and $T_2$ Estimate precisions (a-b) and accuracies (c-d)

**Results:** Table 1 shows the optimized sequence parameters, along with the average TNR efficiencies in the WM/GM region. To numerically verify the validity of the TNR efficiency metric, five thousand independent Monte Carlo trials were repeated for each $T_1/T_2$ pair assuming an expected value of $M_0 = 3000$. Nonlinear least square estimation (NLSE) estimated all $T_1/T_2$ values while including $M_0$ as a nuisance parameter. The Nelder-Mead simplex direct search method minimizes the squared error $\chi^2$ between the simulated noisy and the noise-free data. Converting the TNR efficiency into PCRB (squared root of CRB over $T_1/T_2$) assuming a total scan time of 10 seconds for each relaxometry approach quantifies the predictions on $T_1/T_2$ estimates' precisions. The mean estimation error $\mathrm{MEE} = \sigma(\hat{T}_{1,2})/T_{1,2}$ and the relative bias $\mathrm{Rbias} = (E(\hat{T}_{1,2}) - T_{1,2})/T_{1,2}$ quantify the $T_1/T_2$ estimates' precisions and accuracies, respectively. Fig. 1a demonstrates the $T_1$ estimate MEEs (in dots) against the PCRBs (in dash lines) for $T_1 = [700, 5000]$ ms with reference $T_2 = 85$ ms. Fig. 1b demonstrates the $T_2$ estimate MEEs against the PCRBs for $T_2 = [30, 400]$ ms with reference $T_1 = 1500$ ms. The shaded regions correspond to the WM/GM. Including the larger $T_1$ and $T_2$ ranges examines the estimates' stabilities for diagnosing early brain tissue degenerations and also more advanced damage. Figs. 1c-d show that $T_1$ and $T_2$ are generally over-estimated, but the Rbiases are controlled within [-0.1%, 0.2%] for brain WM/GM regions. The last three columns in Table 1 give the average PCRBs against the average MEEs and Rbiases within the WM/GM $T_1/T_2$ ranges.

Table 1 Optimized sequence parameters and performances for different relaxometry approaches

| Approach | Optimized parameters (ms) | TNR Efficiency | Equi. MC SNR | PCRB (%) | MC MEE (%) | MC Rbias (%) |
|---|---|---|---|---|---|---|
| Conv. IR | TI = [0:450:1800], W = 10000 | $\Gamma_1 = 17.07$ | 42.84 | $P_1 = 1.85$ | $M_1 = 1.86$ | $R_1 = 0.019$ |
| Fast IR | TI = [0:303:2424], TR = 6722 | $\Gamma_1 = 19.57$ | 40.66 | $P_1 = 1.62$ | $M_1 = 1.62$ | $R_1 = 0.0005$ |
| SR | TR = [0:620:6820] | $\Gamma_1 = 7.52$ | 49.43 | $P_1 = 4.21$ | $M_1 = 4.24$ | $R_1 = 0.087$ |
| LL | a = 30°, t = [206:206:3090], TR = 8900 | $\Gamma_1 = 21.32$ | 105.99 | $P_1 = 1.48$ | $M_1 = 1.49$ | $R_1 = 0.009$ |
| SEIR | $TR_{IR} = 2994$, TI = 1270, $TR_{SE} = 2942$, TE = 17 | $\Gamma_1 = 22.56$, $\Gamma_2 = 8.78$ | 117.80 | $P_1 = 1.41$, $P_2 = 3.62$ | $M_1 = 1.41$, $M_2 = 3.63$ | $R_1 = 0.008$, $R_2 = 0.13$ |
| DESPOT | $\alpha_{SPGR} = 8.6°$, $\alpha_{SSFP} = [13.9°, 57.8°]$, $TR_{SPGR} = 6.8$, $TR_{SSFP} = 3.4$ | $\Gamma_1 = 23.29$, $\Gamma_2 = 24.64$ | 2711.63 | $P_1 = 1.36$, $P_2 = 1.28$ | $M_1 = 1.37$, $M_2 = 1.28$ | $R_1 = 0.012$, $R_2 = 0.01$ |

**Discussion and Conclusion:** Both Fig.1 and Table 1 show for all tested relaxometry approaches, the MEEs closely follow the CRB for all tested $T_1$ and $T_2$ ranges. This confirms that the CRB is a tight estimation bound and reliably predicts the $T_1/T_2$ estimation performances. Among all approaches, DESPOT has the highest $T_1$ and $T_2$ estimate efficiency largely due to its very short sequence time, but suffers from a relatively high Rbias and therefore low accuracy in $T_1$ mapping. SEIR, LL and fast IR have similar $T_1$ estimate efficiencies. Conventional IR requires a long sequence time and SR has very low $T_1$ estimate efficiency and therefore are both not recommended for $T_1$ mapping. This is the first time the CRB is utilized in defining the $T_1$ and $T_2$ mapping efficiencies, which provides a consistent and more complete framework evaluating different relaxometry approaches on their $T_1$ and $T_2$ mapping capabilities in quantitative MRI.

**References:** **1.** Bydder et al. J Comput Assist Tomogr 9(4):659-75, 1985. **2.** Gupta et al. JMR 38(3):447-452, 1980. **3.** McDonald et al. JMR 9(3):358-362, 1973. **4.** Look et al. Rev Sci Instrum 41(2):250-251, 1970. **5.** In den Kleef et al. MRM 5(6): 513-524, 1987. **6.** Deoni et al. MRM 49(3):515-526, 2003. **7.** Kay. Englewood Cliffs, NJ: Prentice Hall, 1993. **8.** Edelstein et al. J Comput Assist Tomogr 7:391-401, 1983. **9.** Crawley et al. MRM 7(1):23-34, 1988. **10.** Stanisz et al. MRM 34(3):507-512, 2005.